



Baillet, G. , Denis, A., Bourgoing, A., Magin, T. E. and Laux, C. O. (2021) Passive method to measure reentry radiation in the presence of ablative products. *Journal of Spacecraft and Rockets*, (doi: [10.2514/1.A34969](https://doi.org/10.2514/1.A34969))

The material cannot be used for any other purpose without further permission of the publisher and is for private use only.

There may be differences between this version and the published version. You are advised to consult the publisher's version if you wish to cite from it.

<http://eprints.gla.ac.uk/251418/>

Deposited on 13 September 2021

Enlighten – Research publications by members of the University of
Glasgow

<http://eprints.gla.ac.uk>

Passive method to measure reentry radiation in the presence of ablative products

Gilles Bailet¹

EM2C Laboratory, CNRS UPR288, CentraleSupélec, University Paris Saclay, Gif-sur-Yvette, 91190, France

Amandine Denis²

Aeronautics and Aerospace Department, von Karman Institute for Fluid Dynamics, Rhode-Saint-Genèse, 1640, Belgium

Alexis Bourgoing³

ArianeGroup, Les Mureaux, 78133, France

Thierry Magin⁴

Aeronautics and Aerospace Department, von Karman Institute for Fluid Dynamics, Rhode-Saint-Genèse, 1640, Belgium

and

Christophe O. Laux⁵

EM2C Laboratory, CNRS UPR288, CentraleSupélec, University Paris Saclay, Gif-sur-Yvette, 91190, France

Reentry radiation is one of the key phenomena to take in account while designing an EDL phase for sample return and some gas/ice giants' missions. In the case of an ablative Thermal Protective System (TPS), the physico-chemical processes involved produce a large amount of dust and phenolic gases that can obstruct the optical path. The QARMAN mission (5.2 kg CubeSat launched in December 2019) gave a low-cost opportunity to develop a dedicated payload named INES (Imbedded Nano-platform-size Emission Spectrometer) to study the radiation of a reentry plasma in the presence of an ablative heatshield (Cork P50 from Amorim™). The payload is able to measure both radiation and thickness evolution of the TPS at the same location. The paper presents a passive method to prevent any contamination of

¹ Current affiliation: Research associate. Division of System, Power and Energy. James Watt School of Engineering; gilles.bailet@glasgow.ac.uk

² Research Engineer, Aeronautics and Aerospace Department; denis@vki.ac.be.

³ Research Engineer, Aerodynamics and Atmospheric Re-entry Section; alexis.bourgoing@ariane.group.

⁴ Professor, Aeronautics and Aerospace Department; magin@vki.ac.be.

⁵ Professor, CentraleSupélec ; christophe.laux@centralesupelec.fr.

the optical path from the ablative TPS to be able to measure radiation for a wide range of mission profiles and heatshield locations.

I. Introduction

Among the phenomena encountered during atmospheric entry of a planetary probe, the prediction of plasma radiation remains a significant challenge. When the probe enters the atmosphere, gases are compressed in front of the vehicle, transforming kinetic energy into thermal energy and thus exciting, ionizing, and dissociating the free stream gas. The excited species relax by emitting photons of different energies. If the TPS is of an ablative nature, species such as phenols and other pyrolysis gases are injected into the flow and react with the plasma, thus affecting both the emission and the absorption of radiation. To predict the radiative heat flux, many physico-chemical phenomena need to be described carefully: fluid mechanics, gas chemistry, gas/TPS interaction, emission/absorption of each molecular system/atomic line, and radiative transport. Due to the nature of the radiative process, an uncertainty of 1% in the knowledge of the temperature field typically results in 20 % uncertainty on radiation prediction, especially for air plasmas at equilibrium [1]. Thus, there is a need for flight data and ground-to-flight extrapolation methodology to validate numerical codes in order to reduce uncertainty margins but, unfortunately, radiation and ablation flight data are scarce. Despite the high scientific interest, instrumentation capabilities remain a limitation as they are intrusive and/or do not allow measurements for the full duration of the mission.

In this paper, a dedicated payload named INES (Imbedded Nano-platform-size Emission Spectrometer) is proposed to study the radiation of a reentry plasma in the presence of an ablative heatshield (Cork P50 from AmorimTM). The payload is developed to measure both radiation and thickness evolution of the TPS at the same location. The paper presents a passive method to prevent any contamination of the optical path from the ablative TPS to be able to measure radiation for a wide range of mission profiles and heatshield locations. Section II describes the different strategies used in the past and justifies the need for a low-cost, non-intrusive, in-flight measurement technique. Section III shows an overview of the optical path pollution process. Section IV presents the new instrument able to measure radiation in the presence of ablation in a fully passive method and Section V exposes the performances of this instrument. Finally, Section VI presents the QARMAN flight opportunity, a 5.2 kg reentry CubeSat, and how the instrument is integrated within this platform, as well as perspectives for future missions.

II. Review of Emission Spectroscopy Measurement Techniques

Measurements of radiation in the presence of an ablative heat shield became an intense research topic with the premises of the Apollo program. For the first time in non-military applications, radiative heat fluxes began to be a consideration for TPS sizing. At the time, the Apollo capsule would reach the most constraining reentry conditions ever encountered by a manned spacecraft on the order of $10\text{-}11.5\text{ km}\cdot\text{s}^{-1}$ at 120 km of altitude. At those speeds, the radiative and the convective heat fluxes are of the same order and thus, a clear characterisation of the radiative environment was mandatory for a reliable heatshield sizing leading to an extensive effort of flight data collection to validate models. The following sections expose the various existing techniques and their limitations compared to the solution proposed in this article.

A. Staged windows (FIRE program)

For the Apollo project, the radiative heat flux was identified as one of the key parameters to be measured to ensure the safety of human flight to the Moon. Two testbed missions, named FIRE I&II were proposed [2] to assess radiation at high reentry speed. The FIRE I&II vehicles flew on April 14, 1964 and May 22, 1965, respectively. Direct measurements of the gas radiation in the presence of an ablative TPS were obtained with radiometers during these missions.

Each reentry vehicle consisted of an unmanned vehicle equipped with an onboard computer, batteries, and an acquisition system. In addition, the platform comprised a suite of instruments (calorimeters, radiometers, one spectrometer, pressure probes and thermocouples).

The radiometers were placed at three locations in the reentry vehicle. The first radiometer was positioned at the aft of the capsule to look at the after-body radiation (no ablation contamination expected), the second radiometer was located close to the edge of the front heatshield, and the last one was set to take measurements at the stagnation point. These instruments integrated radiation over the range 200-4000 nm (limit imposed by the fused silica quartz windows used to protect the radiation instruments to the harsh environment). An emission spectrometer with a spectral range of 200-600 nm and 4 nm spectral resolution was also located at the stagnation point of the vehicle. It should be noted that the spectral range of the FIRE II emission spectrometer was limited to 300-600 nm during the flight due to mechanical blockage of the grating. To avoid contamination of the optical path by ablation products, each testbed was equipped with a stack of 3 TPS layers. Before each radiation measurement, a layer of TPS was jettisoned to maximize cleanliness of the optical path. Instrumentation layout and TPS stack's details are presented in Fig. 1.

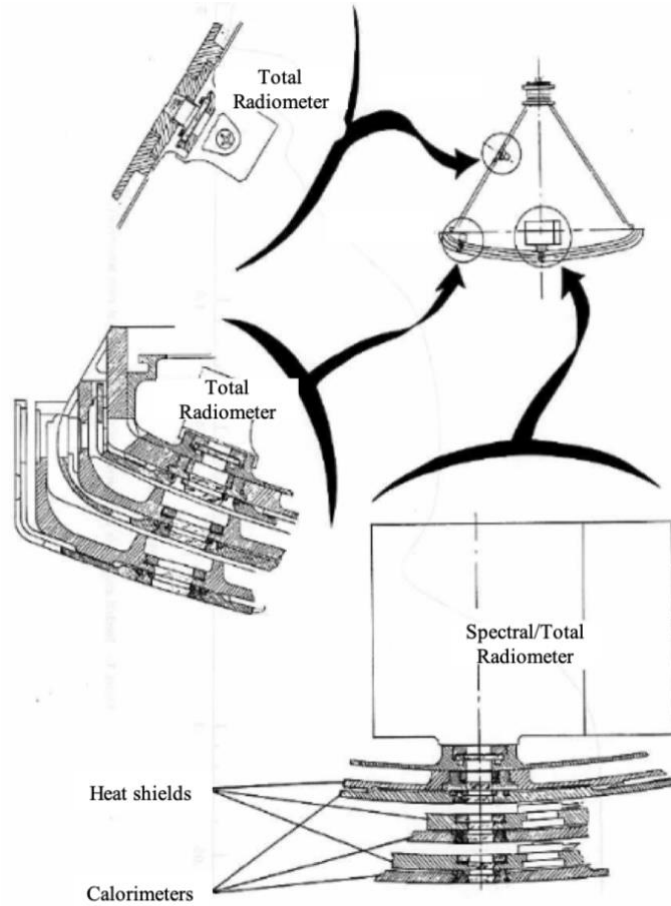


Fig. 1 TPS layers arrangement and Instrumentation location [2].

The use of three stacked TPS layers allowed to have three non-polluted spectra per flight. Tab. 1 summarizes the range of conditions for which measurements were obtained during the FIRE I&II missions.

Table 1 Measurement parameters for the FIRE I&II's radiometers and emission spectrometers

	Data period	Altitude [km]	Velocity [km/s]
FIRE I	1	89.01 – 70.00	11.63 – 11.53
FIRE II	1	83.75 – 69.80	11.37 – 11.30
	2	54.34 – 53.23	10.61 – 10.51
	3	41.80 – 40.75	8.20 – 7.74

The stacked TPS design of the FIRE capsule allows for a non-polluted measurement and prevents a complete blockage by ablation products. However, each time a TPS layer is ejected, the flow is perturbed by the transient phase

of ejection and rebuilding the measurements during that perturbed period is complex. In addition, the TPS layers were composed of a phenolic-asbestos heatshield with imbedded beryllium calorimeters, resulting in the injection of a complex mixture of ablation products into the flow. The large gaps between the measurements and the rebuilt flight predictions were attributed to problems with these calorimeters, and this effect was neither modelled nor characterized [3].

Despite the lack of data and the difficulties of the rebuilding, the dataset obtained in the FIRE program represents as of today the most valuable set of emission spectroscopy measurements in the presence of an ablative TPS for high enthalpy trajectories.

Nevertheless, the method is too intrusive (ejection of TPS layers perturbing the flow) and has a drastic impact on the platform design, thus, this method is not suitable for our use.

B. Conical Canal (Apollo 4/6, COMARS+)

The spectrometer/radiometers instrumentation package on the FIRE I&II platforms imposed significant interface modifications on the capsules, thus preventing its use as a standard and flexible technique. To ease the integration to the platform and avoid perturbation of the flow, Apollo 4/6 and the ExoMars 2016 (COMARS+) used a conical canal as the interface through the TPS (Fig. 2).

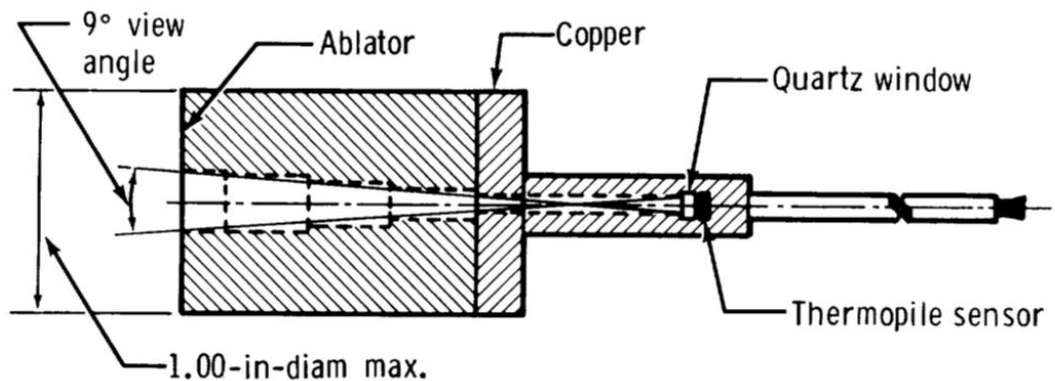


Fig. 2 Conical canal design for the Apollo 4/6's radiometers [4].

Although easier to integrate, this setup can only provide quality measurements for up to 30-45 seconds [5] & [6], whereas the typical measurement time needed to capture the full radiative profile is on the order of 5-20 minutes.

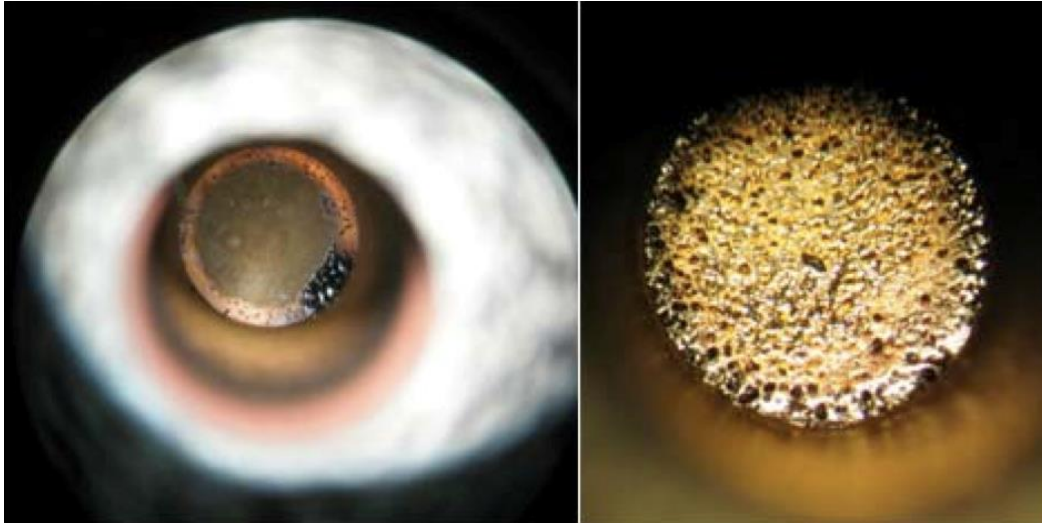


Fig. 3 Impact of optical path pollution in the conventional payload configuration (Left: before test, right: after test of 20-30s duration) [5]

Fig. 3 shows the dust/phenol gas condensate obstructing the optical path at the end of a test carried out in a plasma wind-tunnel for such payload configuration. In these conditions, the measurement is clearly affected by the pollution of the optical path.

C. Flushed Optical Path

The flushed optical path method [7] uses a cavity filled with a neutral gas (typically argon) at a pressure greater than the surface stagnation pressure, thus preventing pollutants from penetrating the optical path.

This method was never tested in flight yet owing to its complexity of integration and its potential to disturb the flow. It requires a tank of neutral gas and an injector, which is difficult to integrate into the platform and to regulate. Moreover, the over-pressurized gas inside the cavity can leak into the shock layer, thus changing the flow and the radiation emitted.

D. Gardon gauge (Mars 2020)

The heatshield of the entry capsule Mars 2020 is equipped with an instrumentation package called Mars Entry Descent and Landing Instrumentation 2 (MEDLI2) [8]. The package incorporates a radiometer (Model 22160-22KS from ©Medtherm Corporation) located at the backshell to measure radiation during Mars entry. Based on a Gardon gauge design, the instrument monitors the temperature of a thermopile (protected by a sapphire window) to sense the radiative heat flux. The protective window is used to avoid direct convective heating of the thermopile. Sapphire

allows for a high and flat spectral transmittivity in the range of interest (190 to 5000 nm). This instrument measures the total radiative flux (190-5000 nm) on the backshell with a field of view of 154° and a measurement range of 0-150 kW/m² covering the expected total peak heat rate of 90 kW/m² [9]. However, even within the small ablation levels occurring at the back shell of the Mars 2020 capsule, arc jet tests [9] have shown a 12-30% loss of signal depending on the TPS material and an expected 20% loss for the Mars 2020 flight profile.

E. Summary

Through this review of the existing instruments able to measure radiation in the presence of ablation, we have identified a need for a system that is easy to integrate, does not perturb the plasma flow, and suffers minimally from contamination products. The next section explores the contamination process and proposes a solution that is a variant of the conical canal.

III. Optical Path Contamination during Radiation Measurement

To perform accurate spectroscopic measurements in an ablative environment, the mechanisms of optical path pollution must be understood. To this end, ablative samples (Cork P50 [11]: Cork + Phenolic Resin) were exposed to a plasma flow obtained in the VKI Plasmatron facility [11]. The facility is equipped with a 160 mm diameter inductively coupled plasma torch powered by a 400 kHz frequency, 1.2 MW power, and 2 kV voltage generator. The gas is heated by induction through a coil, creating a high-purity plasma flow. For the results presented here, atmospheric air at a mass flow of 16 g/s is used to produce a subsonic plasma flow. The static pressure in the chamber is 10 mbar. Tests were conducted in various regimes corresponding to a low Earth orbit type reentry trajectory (heat fluxes between 0.5 and 3 MW/m²).

A. Test setup

In this section, we present a testing campaign performed with the conventional design (conical canal) found in the literature (Fig. 2, [6]). The optical access is located at the bottom of a metallic cylinder, itself located below a protective layer of TPS. This design has been shown to be efficient only for a limited time period as the optical path is blocked after 30-45 seconds of use [5]. To assess the physical phenomenon involved, the test is performed with the probes presented in Fig. 4 and Fig. 5 following two phases.

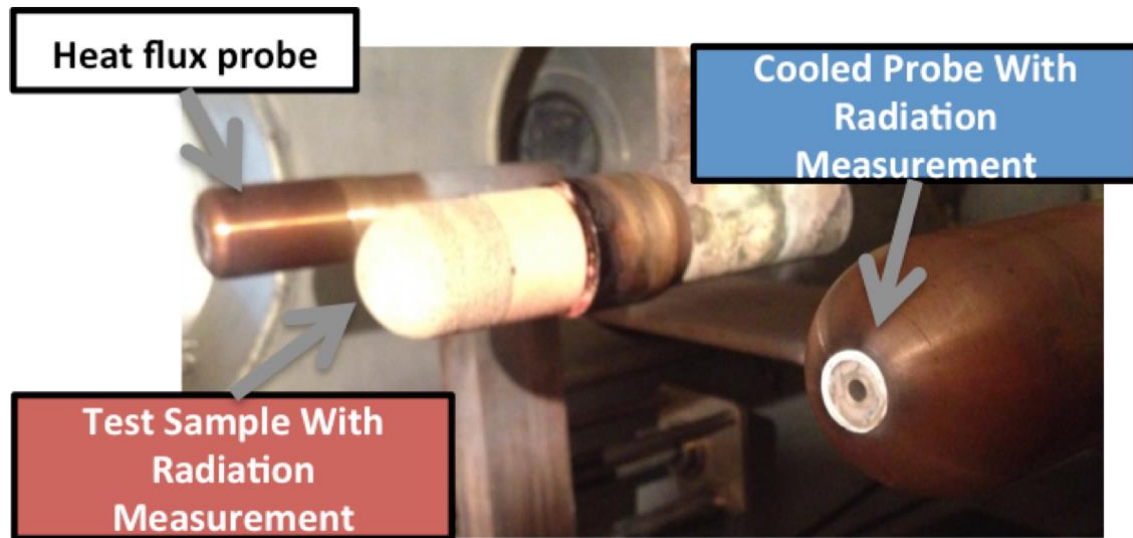


Fig. 4 Dual probe measurement set up [12].

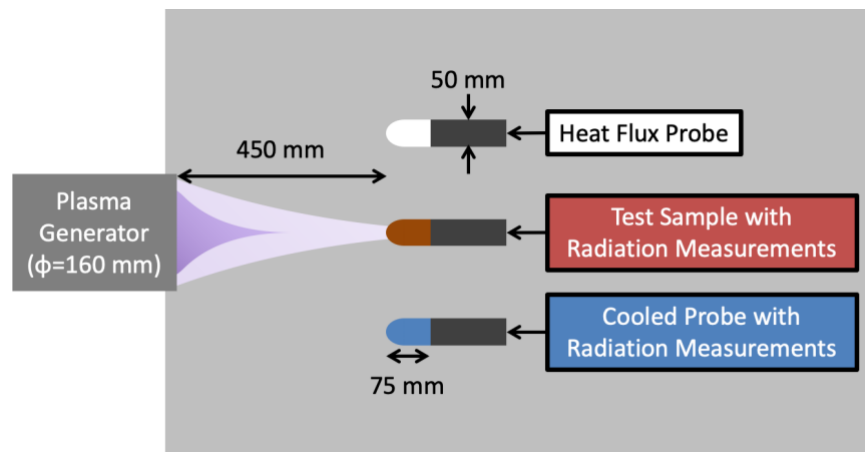


Fig. 5 Top view and dimensions of the dual probe measurement set up.

The stagnation point heat flux is first measured by means of a water-cooled calorimeter. After reaching the target operating conditions (mass flow rate, static pressure, and cold-wall heat flux), a cooled probe (right on Fig. 4) is inserted into the plasma jet using a pneumatic mechanism to measure the radiation on the stagnation line. The temperature of the probe wall is kept constant at 350 K. It is assumed that the boundary layer does not emit or absorb radiation linked with ablation phenomena in the studied wavelength range [190-1100] nm. Thus, this technique allows us to measure the radiation coming from the ablation process.

The second phase of the test starts with the insertion of a second radiation measurement probe (middle on Fig. 4) in place of the cold probe. The surface of the probe is covered with the TPS material of interest. In the present case, the probe is built with the conical design for the canal (Fig. 2) covered with a Cork P50 ablative material. In

comparison with the first phase, the Cork P50 wall reaches high temperatures, while the boundary layer contaminated by ablation products emits and absorbs radiation. The TPS material also produces phenolic gases and ablation dust (due to erosion and spallation) that may obstruct the optical path.

Using both the cold and ablative radiative probes, one can identify the contribution of the TPS to the total radiative flux and understand the mechanism of optical path pollution. We call this method the dual spectral measurement. In this paper, we focus only on the total radiative flux measured with the conventional design to illustrate the optical path pollution, additional details are given in [12] and [13].

B. Contamination test results

The contamination process of the conventional probe described in Fig. 2 is now investigated using the Plasmatron facility with testing conditions set at 0.5 MW/m^2 for the heat flux and 10 mbar for the static pressure. These relatively low power settings were chosen to enable a slower build-up of the optical path pollution in order to track its evolution. The measurement lasted 3 minutes until full blockage of the optical path, while its contamination by ablation products appeared already after 30s. Fig. 6 shows the integrated spectral intensity measured during the test.

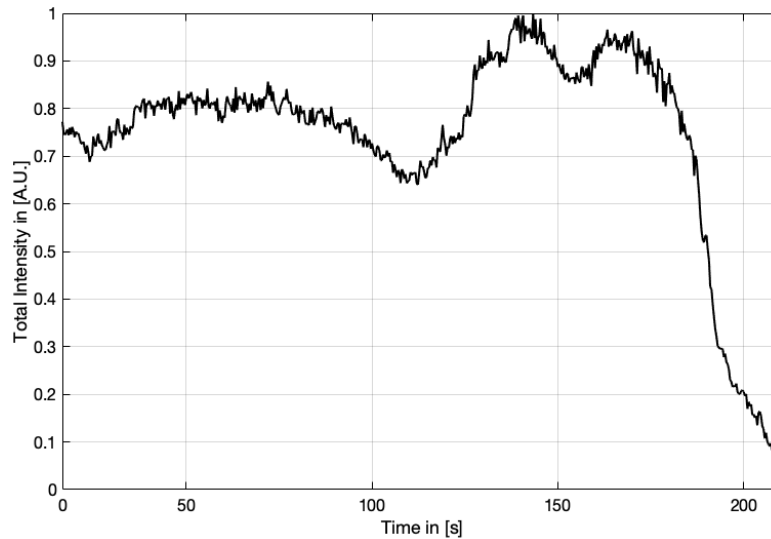


Fig. 6 Total intensity measured with the conventional design. The variations in time show the drastic effect of optical path pollution (heat flux: 0.5 MW/m^2 , static pressure: 10 mbar).

In addition to the radiation measurements, the Cork P50 probe is equipped with thermocouples (TC) monitoring the temperature of the TPS both in front and behind the protective sapphire window, as show in Fig. 7.

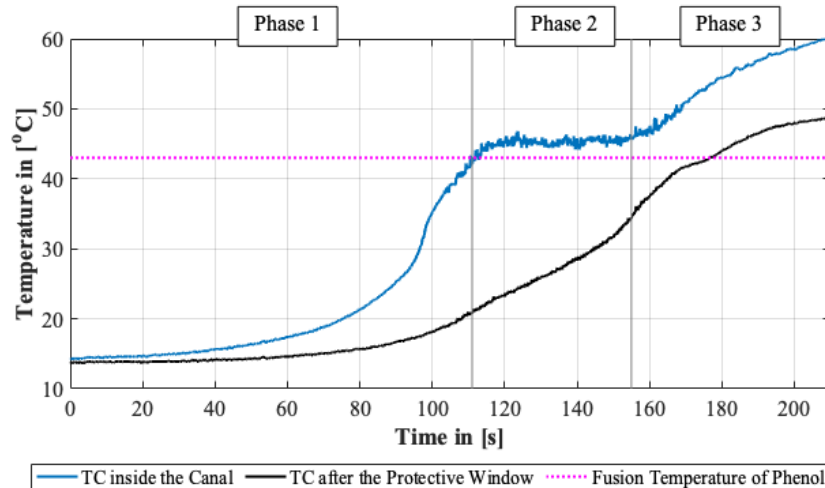


Fig. 7 Temperature profile at the front and back of the protective sapphire window during the Plasmatron test (heat flux: 0.5 MW/m^2 , static pressure: 10 mbar).

Three distinct phases can be identified for the temperature measurement by means of the TC inside the canal corresponding to a first temperature increase, a plateau and a second temperature increase. Looking at the first phase ($t < 111\text{s}$), we can deduce that the intensity measured in Fig. 6 is relatively constant until the phenol starts melting in the canal near the surface. During the phase 2 ($111\text{s} < t < 155\text{s}$), the temperature measured reaches a plateau corresponding to the fusion temperature of phenol (43°C). Melting and sublimation of phenol enhances the concentration of ablation products that participate to the radiative processes in the boundary layer around the sample. During the phase 3 ($t > 155\text{s}$), the phenol decomposition is assumed to be ended, the TC measurement shows an increase in temperature associated to the thermal degradation of other TPS components and some additional contamination of the sapphire window, which would explain the drastic drop of intensity measured at the end of the test.

Indeed, a post-testing inspection of the protective sapphire window (Fig. 8) shows transparent brownish droplets and dark particles. The transparent brownish droplets correspond to pyrolysis gas condensates produced during the initial phases of the optical path contamination, starting at $T > 43^\circ\text{C}$. The dark particles are produced by erosion of the char layer in Phase 3. After the test, some air flow might also enter the canal carrying along some additional particles.



Fig. 8 Photograph of the protective window after the Plasmatron test (heat flux: 0.5 MW/m^2 , static pressure: 10 mbar).

Finally, we should mention that with the conventional system at low heat flux, no chemical ablation was observed but pyrolysis contamination occurred until total obstruction of the optical path. This harsh pollution is due to the low heat fluxes needed for the TPS surface to reach 43°C . So even for Mars entry and an instrument located on the back shell (low ablation), obstruction of the optical path is expected with conventional strategies.

The following section presents an alternative design making possible to perform contamination-free radiation measurements over a wide range of entry/reentry conditions in a passive and non-intrusive manner.

IV. Passive Method to Minimize Optical Path Pollution

A. Design of the canal/cavity

In this section, we present a novel design able to alleviate the shortcomings of the traditional designs. This design can be used on any entry/reentry platform. This new system is patented by ArianeGroup [14]. A schematic of the design is presented in Fig. 9.

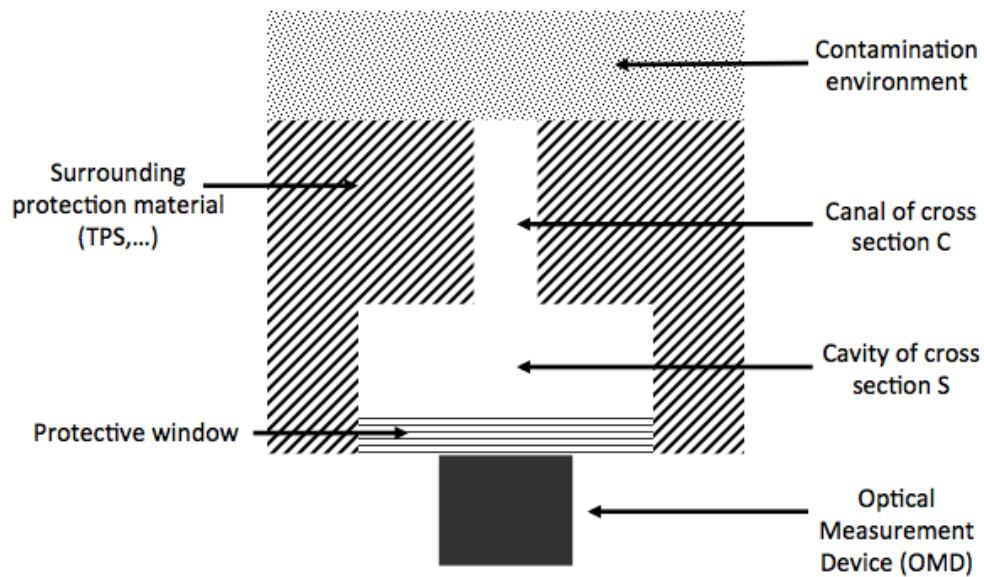


Fig. 9 Schematic of the proposed design.

As shown in Fig. 9, the instrument is composed of two hollow parts, a long canal (diameter C) within the TPS material and a cavity (diameter S) between the canal and the Optical Measurement Device (OMD). A transparent window can be located between the cavity and the OMD to protect the instrument. For maximal wavelength coverage, a sapphire window is recommended.

In this design, it is important to choose the canal diameter C to be much smaller than the cavity diameter S . A ratio “ S/C ” of 5 has been selected for the design presented in this article. This configuration provides two benefits:

- 1) A pressure oscillation is created in the system as in other kinds of forward-facing cavities [15]. Amplified by the canal/cavity specific geometry, it prevents the ablation products from reaching the protective window.
- 2) The large S/C ratio reduces the flux per unit area of particles/phenolic gas that might still enter the cavity despite the adverse pressure gradient.

This system greatly reduces or even eliminates pollution of the optical path, even at high enthalpy conditions. If residual pollution is still present, a slightly larger and longer cavity is expected to solve the issue. In all our tests, no change in canal diameter was observed and no melted flow or debris entered it. These results were obtained for a wide range of TPS materials (PTFE, Cork P50, Graphite, and ASTERM), gas mixtures (air, N_2 , and CO_2), and cold-wall

heat fluxes ($<100 \text{ kW/m}^2$ to 3 MW/m^2). Further tests are needed to confirm the validity of these observations, but the current range encompasses most foreseen missions for Mars entry and Earth LEO reentry.

B. Design optimization

The design was optimized in a flight-relevant environment using the boundary layer duplication methodology presented in [16] and a hemispherical test sample. In this section, various canal/cavity geometries are tested and compared with the state-of-the-art design (simple conical canal).

Fig. 10 shows the cross-section of the probe with the different components and design parameters (canal diameter C , cavity diameter S , and cavity height h). An optical fiber is connected outside the probe to an emission spectrometer for characterization of the radiative intensity and the possible contamination by ablation products.

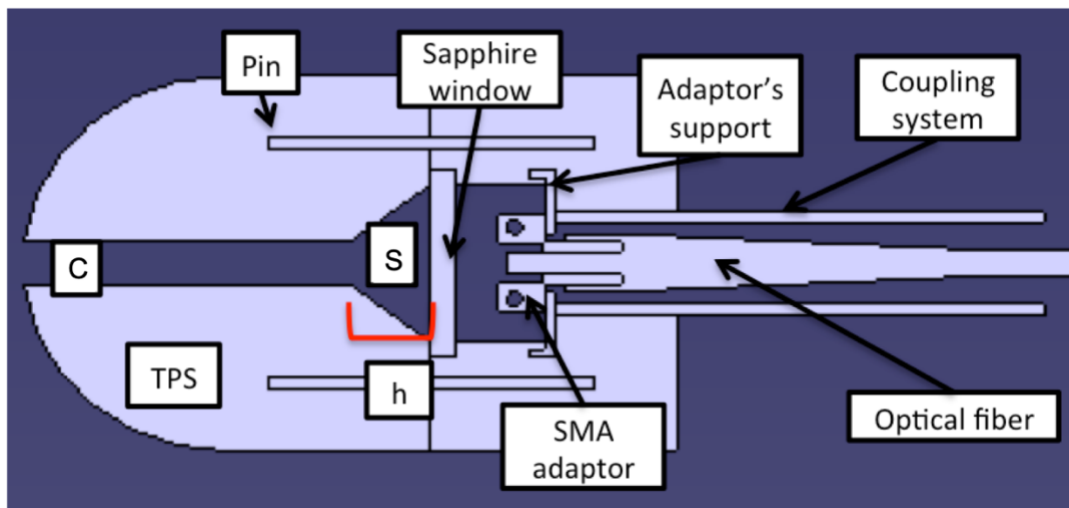


Fig. 10 Probe for design optimization

During the test campaign, two types of cavities were used. The first cavity type is conical, with a 45-degree cone angle and a 20-mm base diameter. The second cavity type is cylindrical.

The preliminary test campaign included 12 tests in the conditions reported in Tab. 2. The first part of the table corresponds to the tests performed with the low power Minitorch [17] and the second part to those performed in the Plasmatron. For each test, a specific geometry of the cavity/canal is defined. The relevant parameters C , S , and h are defined in Tab. 2.

To assess the performance of each cavity/canal configuration, we define the Effectiveness Time (ET) as the time duration for which no major contamination was detected. For some of the tests, the limit of the ET was not contamination but end of the test, due to full sample recession. In this case, the Extinction column will be noted as “NO”.

For the Minitorch case, the test conditions were not determined precisely using a water-cooled calorimeter. In this case, we performed a qualitative test for all configurations at the same location.

In the case of the Plasmatron, we chose the following test condition: heat flux = 1.5 MW/m², static pressure = 100 mbar. With a hemispherical 5-cm diameter test sample, this test condition gives a point of comparison to representative peak heat flux conditions of a LEO return trajectory.

Table 2 Cavity geometries and performances for the design convergence test campaign

Minitorch Test Campaign					
Test Number	Cavity Configuration in [mm] see Fig. 10			ET in [s]	Extinction
	C	S	h		
1	6	6	0	130	YES
2	4	4	0	325	YES
3	2	2	0	383	YES
4	4	20	10	525	NO
5	2	20	10	405	NO
7	4	20	5	496	NO
8	4	10	10	440	NO
Plasmatron Test Campaign (heat flux = 1.5 MW/m ² , static pressure = 100 mbar)					
Test Number	Cavity Configuration in [mm] see Fig. 10			ET in [s]	Extinction
	C	S	h		
6	4	4	0	170	YES
9		Conical (D=20)		190	YES
10		Conical with Eccoband 285 (D=20)		185	YES
	4	20	10		
11		Cylindrical with Kapton tape coating		245	NO
12		Cylindrical with metallic casing		230	NO

At the end of this test campaign, the canal geometry was chosen as illustrated in Fig. 11. The design parameters are the following: canal diameter C = 4 mm, cavity diameter S = 20 mm, cavity height h = 10 mm and canal height of 40 mm. In the last validation case, a metallic casing (titanium) was installed to isolate the cavity from the TPS.

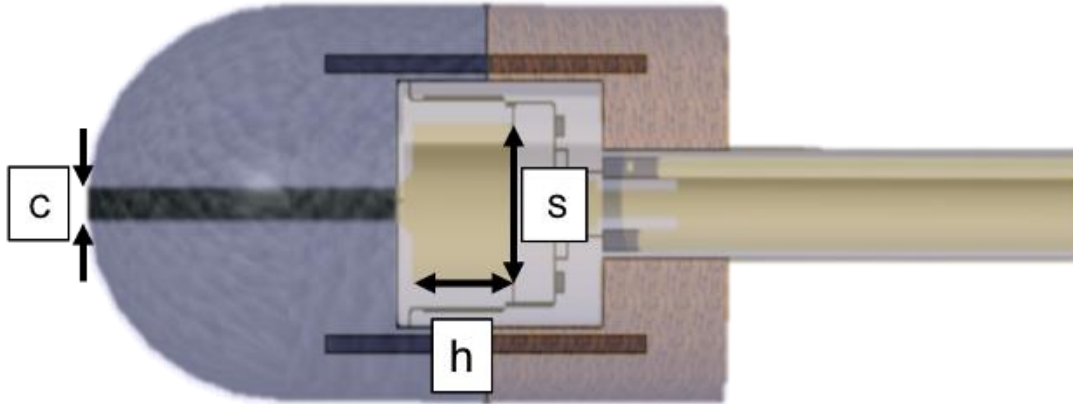


Fig. 11. Final canal/cavity design used during the follow-up tests and the payload design (grey/copper); embedded inside the TPS sample (dark: test article; brown: protective afterbody).

The following section presents the results of a second test campaign with the design presented in Fig. 11 and validated on test 12 (Tab. 2).

C. Sensor selection

As for any optical measurement device performing measurement through the thermal protection system (Staged window, Apollo 4/6, COMARS+), the field of view is highly constrained. To ensure proper measurement, it is necessary to select an appropriate sensor. A CCD (Charge-Coupled Device) based sensor is recommended. This type of sensor allows us to improve the signal-to-noise ratio by increasing the integration time. Associated with a suitable acquisition system, it is possible to cover the full measurement range with sufficient signal. For the QARMAN CubeSat described in Section VI, the selected sensors allow us to perform measurement during the reentry starting at 80 km. Increasing the acquisition time to 1 second, it is possible to perform measurements starting at 120 km for the LEO reentry, thus allowing measurements of low-pressure reentry plasma.

V. Performance of the Measurement Technique

The payload was tested for the QARMAN reentry heating conditions (see section VI, heat flux between 0.5 and 3 MW/m² for a static pressure of 10 to 100 mbar). In all cases, no pollution was observed from ablation or pyrolysis products. Visual inspection of the protective windows showed no deposition whatsoever. Fig. 12 shows an example of the radiative measurement for the peak radiative flux of the QARMAN mission. The measurements were performed

in the ICP torch, with a heat flux of 3 MW/m^2 and a static pressure of 100 mbar [18]. No pollution was observed and the sensor captured the full radiative flux. The slight variations around the nominal level are due to small changes in the power of the ICP torch.

Additionally, due to the heating of the TPS, black body radiation coming from the canal and cavity had to be investigated. A conservative simulation considering the worst-case scenario and a full char layer at 2500 K gave a maximal expected black body radiation of the canal and cavity of $7.4 \cdot 10^{-13} \text{ W/m}^2$ in the spectral range of interest during the ICP test (190-1200 nm) and $2.4 \cdot 10^{-13} \text{ W/m}^2$ for the full range of transmission of the protective sapphire window (below 5000 nm). This amount of radiation represents 0.4% of the predicted free flow radiation. Moreover, analysis of the experimental results showed no measurable contribution of the canal and cavity black body radiation. Therefore, we do not consider this effect further in the rest of the section.

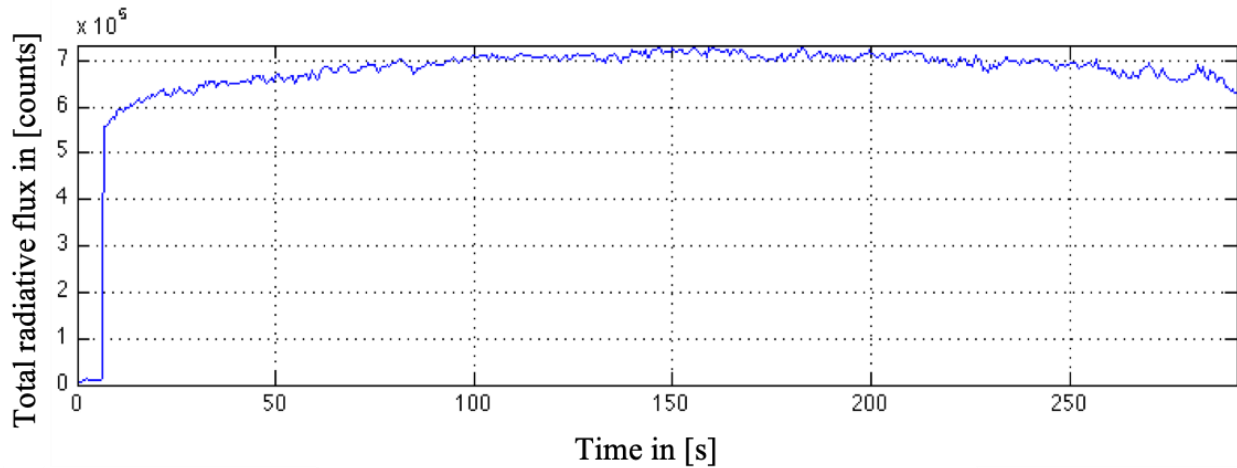


Fig. 12 Radiative flux measured during the Plasmatron test (no optical path pollution observed).

At this heat flux and pressure conditioned, the conventional design was able to measure “contaminated signal” for about 35 seconds only. In contrast, the canal/cavity configuration was able to measure the signal during the full length of the test (i.e. 5 minutes). The duration of the test was only limited by the size of the sample tested, which was totally ablated.

An additional set of tests was conducted to explore the potential of the canal/cavity set up for other trajectory/mission profiles (Lunar return and Mars entry). Fig. 13 show the tested probes during a low energy reentry with PTFE TPS (heat flux= 300 kW/m^2), a high energy type lunar return reentry with graphite TPS (heat flux> $>3 \text{ MW/m}^2$) and a Mars type entry with Cork P50 (heat flux= 2.6 MW/m^2).

In all cases, the instrument was able to capture the full radiation without any sign of contamination. Depending on future missions (Venus, Mars, Titan, Giants), a more extensive flight campaign will be conducted to fully qualify the instrument for the new flight regimes.

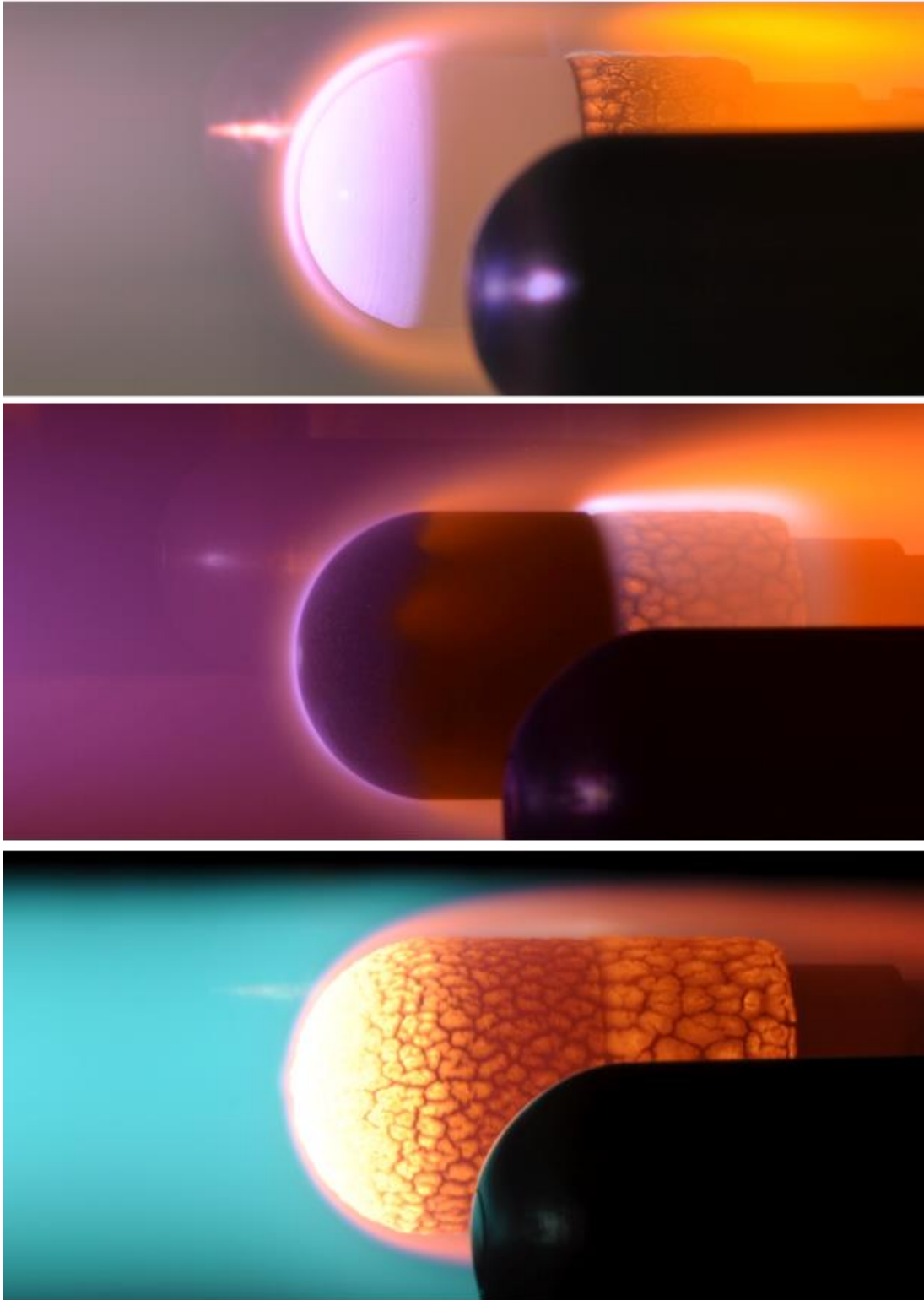


Fig. 13 Test of the canal cavity design for different mission profiles (top to bottom: low ballistic coefficient PTFE heat flux=300 kW/m²; Lunar Return Type reentry with graphite; Mars Entry with Cork P50)

VI. Flight Opportunity: QARMAN mission

A. Flight Opportunity

The new system presented in this paper is part of the INES (Imbedded Nano-size Emission Spectrometer) instrument which allows us to measure reentry plasma radiation without optical path pollution at the same location (same optical access) as the measurement of the TPS shape change (both recession and swelling). This instrument was installed on QARMAN (QubeSat for Atmospheric Research and Measurement on Ablation), a 5.2 kg reentry platform (34x10x10 cm³, fitting the CubeSat standard) with a TPS made of cork P50 (Amorim™). It is the first CubeSat designed to survive atmospheric reentry. The goal of the QARMAN mission is to demonstrate the usability of a CubeSat as an atmospheric entry vehicle. QARMAN has been in space since February 9, 2020 when it was deployed from the International Space Station and is expected to reenter Earth's atmosphere in January 2022.

B. Emission Spectrometer

INES is highly constrained in mass and volume, therefore a trade-off has to be made to obtain the highest possible science return with minimal impact on the QARMAN platform. Commercial Off-The-Shelf (COTS) instrumentation was used to reduce development costs.

A summary of the radiative phenomena to be investigated by the INES instrument is presented in [13] and the main spectral radiation features of interest are plotted in Fig. 14. A summary of the features (weight, spectral range, spectral resolution) of preselected COTS emission spectrometers fitting the allocated mass and volume budgets is also presented.

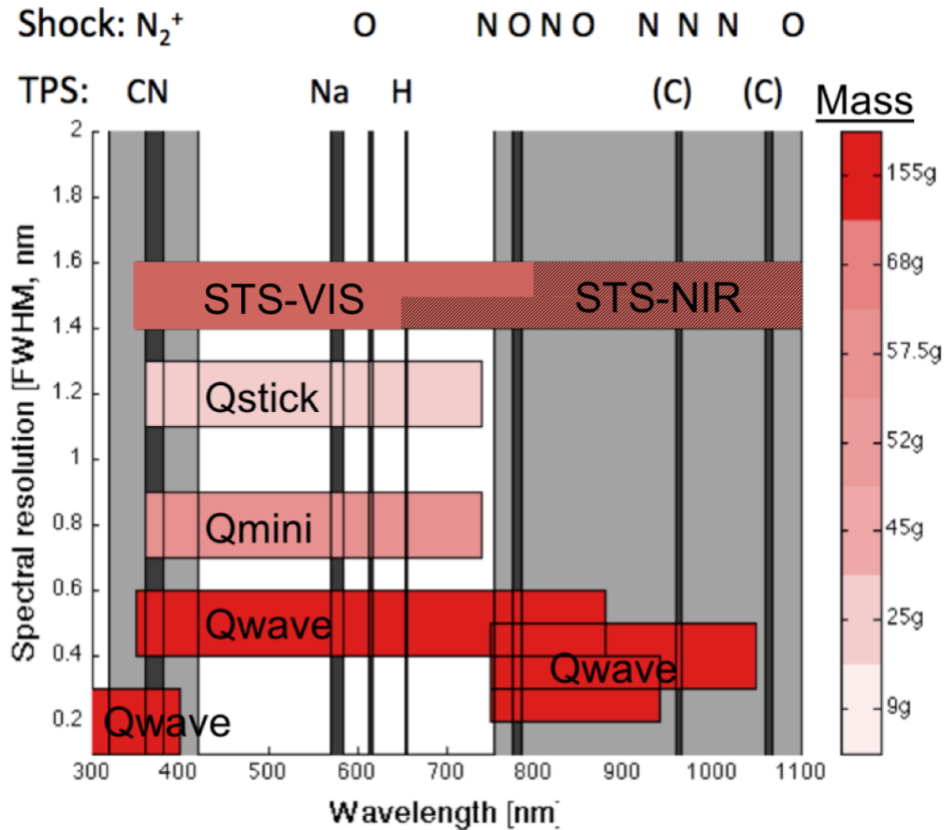


Fig. 14 Summary of the available instrumentation for the wavelength ranges of interest. (red scale: spectrometer weights; light grey: radiation from air plasma; dark grey: radiation from ablation products).

The Ocean-Optics STS-VIS [19] was chosen for its wide wavelength coverage (350-800 nm), small mass (68 g), and small volume (42x40x25 mm³). However, the STS-VIS spectrometer is not flight compatible as such. Vibrations during the launch or reentry phases are likely to break/unalign the optics. To secure the positions of the CCD, grating and mirrors, we developed a specific gluing process (Fig. 15). Two glues (EP37-3FLFAO [20] and EP30-3LO [21]) were selected for their low-outgassing characteristics (space certified for NASA).

EP30-3LO is optically clear and rigid once cured (red in Fig. 15). It is used to fix illuminated parts of the optics that should not move to remain aligned (entrance slit, grating, mirrors, CCD detector) and as positioning anchors. The EP37-3FLFAO, a flexible glue, is able to absorb strains and loads (blue in Fig. 15) to dissipate the energy of vibrations, shocks, and thermal expansion. Fig. 15 shows the location of the two glues inside the STS-VIS spectrometer, and Fig. 16 shows close-up pictures of the glueing of the optical side.

A vibration test (“environmental test”) of the payload was successfully performed, showing no damage to the full instrument, and post-vibration testing showed that the nominal performances were preserved.

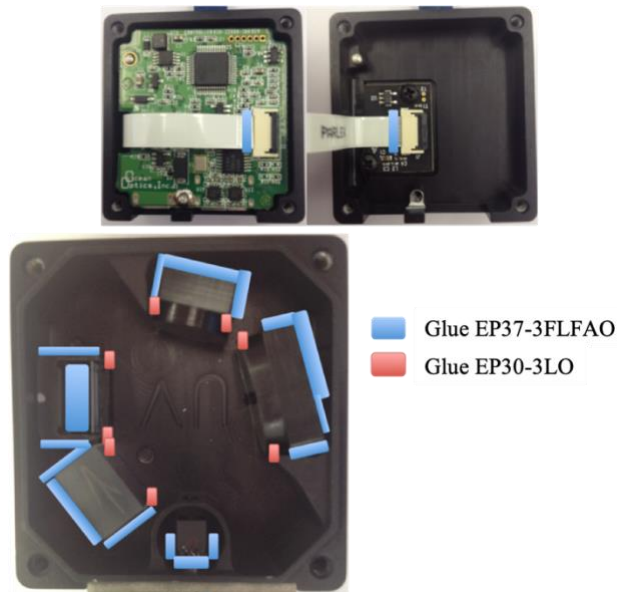


Fig. 15 Areas of glue application in the STS-VIS spectrometer (top: electronic side; bottom: optics side).
 Clockwise from bottom: Entrance slit, grating, CCD detector, mirror 1, mirror 2.

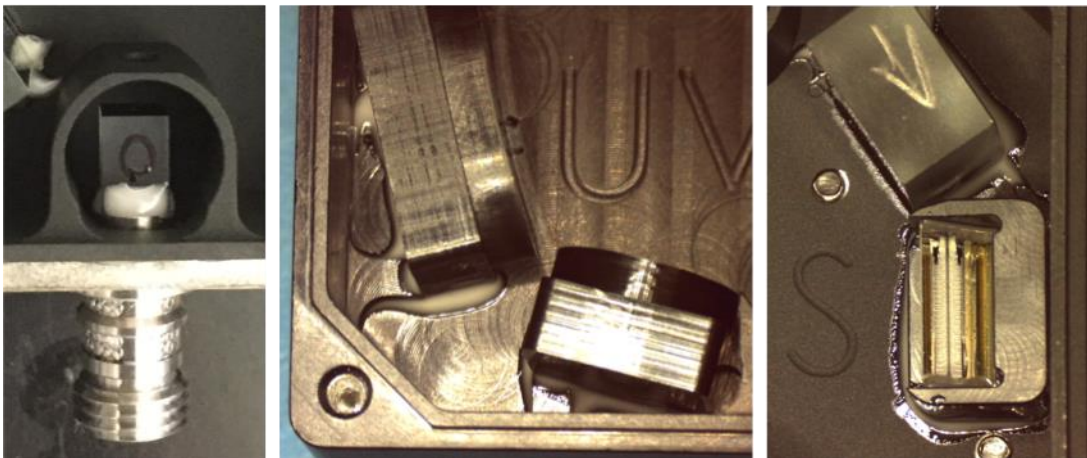


Fig. 16 Glue applied on the INES' optics (from left to right: slit, mirrors, grating and CCD).

C. INES Instrument Setup

The INES instrument using the canal and cavity setup presented in this paper (cross section in Fig. 17) has a total mass of 350g for a volume of $\Phi 31 \times 89 \text{mm}^3$. This design is particularly well suited for entry/reentry platforms in need of an efficient and flexible radiation and TPS thickness measurement payload. In addition of the STS-VIS, the various components include a FDS-010 [22] photodiode, a BSW25 [23] beam splitter, and a WG31050 [24] sapphire window, all from Thorlabs. These components were selected for their performances, reliability and low-cost.

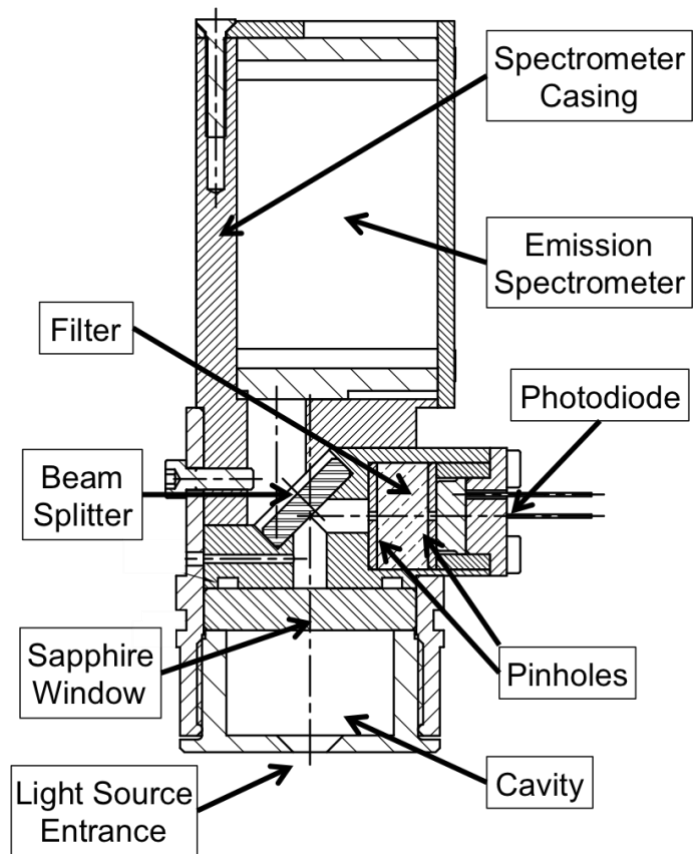


Fig. 17 Cross-section of the INES payload and its components

To satisfy launch and reentry constraints, the structure of the payload is made of machined titanium. Fig18 shows a photograph of the flight instrumentation hardware prior to final integration.

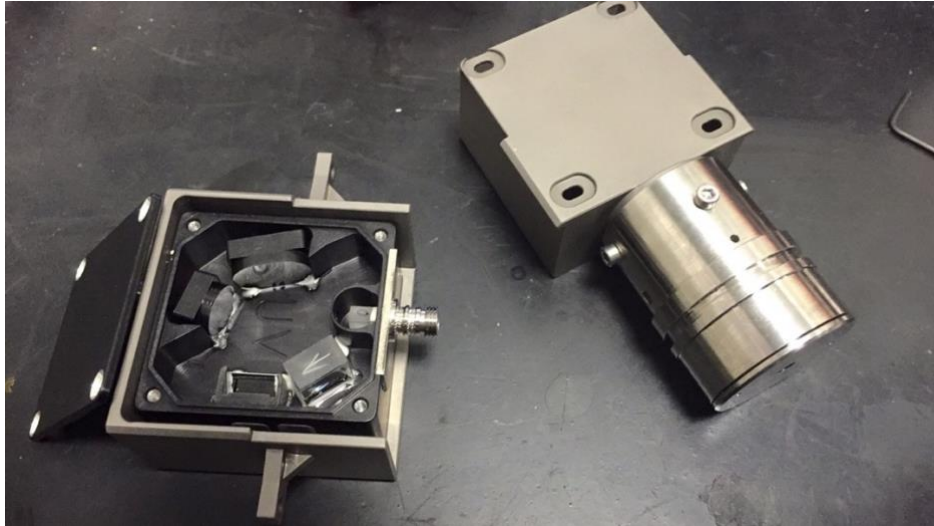


Fig. 18 Full payload prior to final assembly for pre-flight testing (left: emission spectrometer casing; right: smart plug casing).

D. Mini-INES-Grad Configuration

Planetary exploration vehicles tend to be highly constrained in terms of the mass, volume, data acquisition and data storage available for science objectives. In order to propose a solution for the most constrained platforms, a simpler version of INES can be developed where only the total radiative flux is measured (Fig. 19). This application is useful when no recession is expected (Titan entry) and when mass is extremely limited. With a mass of only 100g, the Mini-INES-Grad is the smallest instrument available. It includes the full metallic casing (with the included canal/cavity), a photodiode, and a small board for the data acquisition system.

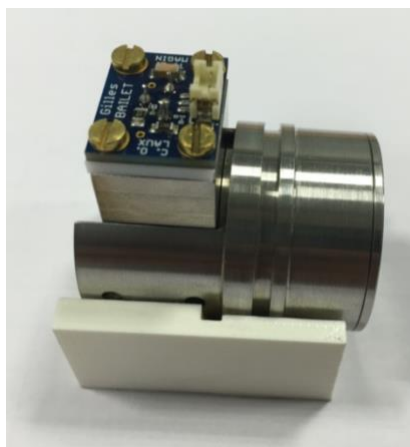


Fig. 19 Mini-INES-Grad configuration

VII. Conclusion

The limitations of current instruments, in terms of bulkiness and/or intrusiveness, were discussed. The issue of optical path contamination, which affects many existing instruments and prevents reliable measurements, was solved with a novel approach. First, we measured the temperature field inside the canal between the plasma and the spectrometer. We observed that, above a threshold temperature of 318 K, most common materials (cork and/or phenolic resin based) start outgassing, thus reducing the optical transparency of the canal. To overcome this problem, we conducted an extensive investigation of canal/cavity geometries to keep the temperature of the walls of the optical path below 318 K, and thus prevent the production of dust that could deposit on the optics.

A new instrument capable of measuring emission spectra without suffering from dust contamination was then proposed. An optimisation of the design parameters was performed thanks to an experimental testing campaign. Preliminary plasma tests showed that the instrument would be suitable for more extreme conditions and entry on other celestial bodies. The final configuration was qualified for a LEO return type reentry and its integration within the QARMAN flight opportunity was presented.

The full flight instrument, called INES (Imbedded Nanosize Emission Spectrometer), weighs 350 g, including a 68-g emission spectrometer (336-822 nm spectral range with a resolution of 1 nm) and a 5-g photodiode (777 nm). The spectral range of the spectrometer was selected based on the features of interest from the ablation process. A mini-INES configuration was also presented, weighing 150 g, with only two photodiodes for total radiative flux and recession/sublimation/swelling measurements. This instrument is also described in 2 patents owned by ArianeGroup ([14] and [25]) and efforts are ongoing to propose the instrument for future missions. Finally, we presented an even lighter configuration (Mini-INES-Grad weighing only 100 g) that can measure the total radiative flux with only one photodiode without any contamination of the optical path.

Acknowledgments

GB has received funding for this work from the ANRT with the ArianeGroup CIFRE grant #0064/2013 and the QARMAN project was supported by an ESA GSTP grant #4000109824/13/NL/MH.

References

- [1] C. O. Laux, "Optical Diagnostics and Radiative Emission of Air Plasmas," Stanford University, 1993.

- [2] D. L. Cauchon, "Radiative Heating Results from the FIRE II Flight Experiment at a Reentry Velocity of 11.4 Kilometers per Second," NASA, TM-X1402, 1967.
- [3] F. Mazoue and L. Marraffa, "Determination of the Radiation Emission during the Fire II Entry," in *2nd International Workshop on Radiation of High Temperature Gases in Atmospheric Entry*, Rome, 2006.
- [4] R. C. Ried Jr, W. C. Rochelle and J. D. Milhoan, "Radiative Heating to the Apollo Command Module Engineering Prediction and Flight Measurement," NASA technical report, TM X-58091, 1972.
- [5] A. Preci, N. Eswein, G. Herdrich, S. Fasoulas, H.-P. Roser and M. Auweter-Kurtz, "Development of a Combined Sensor System for Atmospheric Entry Missions," in *Proceedings of the 7th European Symposium on Aerothermodynamics*, Brugge, 2011.
- [6] A. Gülhan, F. Siebe and T. Thiele, "Combined Sensor Assembly COMARS for EXOMARS EDM Demonstrator," in *9th International Planetary Probe Workshop*, Toulouse, 2012.
- [7] K. Neidhard, H. Kalippke, F. Wendel, E. Renninger, W. Staudemaier, J. Meiwes, A. Gerhard, D. Dick and H. Becker, "Flowing Gas Seal Enclosure for Processing Workpiece Surface with Controlled Gas Environment and Intense Laser Irradiation". USA Patent WO1991002893A1, 07 03 1991.
- [8] H. Hwang, D. Bose, H. Wright, T. R. White, M. Schoenenberger, J. Santos, C. D. Karlgaard, C. Kuhl, T. Oishi and D. Trombetta, "Mars 2020 Entry, Descent, and Landing Instrumentation (MEDLI2)," in *46th AIAA Thermophysics Conference*, 2016. <https://doi.org/10.2514/6.2016-3536>
- [9] R. A. Miller, C. Y. Tang, M. S. McGlaughlin, T. R. White, T. S. Ho, M. E. MacDonald and B. A. Cruden, "Characterization of a radiometer window for Mars aftbody heating including ablation product deposition using a miniature arc jet," in *2018 Joint Thermophysics and Heat Transfer Conference*, 2018. <https://doi.org/10.2514/6.2018-3590>
- [10] B. Helber, O. Chazot, A. Hubin and T. Magin, "Emission spectroscopic boundary layer investigation during ablative material testing in plasmatron," *Journal of Visualized Experiments*, pp. AIAA 2012-2876, 112: e53742, 2016. <https://dx.doi.org/10.3791/53742>
- [11] Amorim Cork Composites, "Reinventing Thermal Protection in Aerospace Applications," 04 07 2008. [Online]. Available: https://www.amorimasia.com/uploads/4/8/0/0/48004771/tps_pp_04_07_2008ac.pdf. [Accessed 15 09 2020].
- [12] G. Bailet, A. Bourgoing, T. Magin and C. O. Laux, "New method of predicting reentry radiation on the presence of a non-conventional / non-characterized thermal protection system material," in *13th International Planetary Probe Workshop*, Laurel, 2016b.
- [13] G. Bailet, *Radiation and ablation studies for in-flight validation*, CentraleSupélec, University Paris-Saclay, 2019.
- [14] G. Bailet, "Apparatus reduction liability of pollution of an optical access of an optical instrument". WO Patent WO2018100255A1, 07 06 2018a.
- [15] J. Kim and S. S. Park, "Unsteady characteristics of hypersonic forward facing cavity flow," in *18th Applied Aerodynamics Conference, Fluid Dynamics and Co-located Conferences*, Denver, USA, 2000. <https://doi.org/10.2514/6.2000-3925>
- [16] Barbante, P.F., Chazot, O., Flight extrapolation of plasma wind tunnel of stagnation region flowfield, *J. Thermophys. Heat Transfer*, July – September 2006, Vol.20, No.3, pp 493-499. <https://doi.org/10.2514/1.17185>
- [17] G. Degrez, D. Abeele, P. Barbante and B. Bottin, "Numerical simulation of inductively coupled plasma flows and hypersonic (RE-)entry flows," in *European Congress on Computational Methods in Applied Sciences and Engineering*, Barcelona, 2000.

- [18] G. Bailet, T. Magin and C. O. Laux, "Reentry Platform for Studying Radiation, from Payload Design to Performances," in *Summaries of VKI's doctoral candidate research 2015-2016*, 2016.
- [19] Ocean Optics, 2018. [Online]. Available: <https://www.oceaninsight.com/products/spectrometers/microspectrometer/sts-series/sts-uv/>. [Accessed 2018].
- [20] MASTERBOND, "EP37-3FLFAO Product Information," 2018a. [Online]. Available: <https://www.masterbond.com/tds/ep37-3flfao>. [Accessed 10 10 2018].
- [21] MASTERBOND, "EP30-3LO Product Information," 2018b. [Online]. Available: <https://www.masterbond.com/tds/ep30-3lo>. [Accessed 10 10 2018].
- [22] Thorlabs, "FDS010 - Si Photodiode, 1 ns Rise Time, 200 - 1100 nm, Ø1 mm Active Area," 2018. [Online]. Available: <https://www.thorlabs.com/thorproduct.cfm?partnumber=FDS010>. [Accessed 10 10 2018].
- [23] Thorlabs, "BSW25 - Ø1/2" 50:50 UVFS Plate Beamsplitter, Coating: 350 - 1100 nm, t = 3.0 mm," 2018. [Online]. Available: <https://www.thorlabs.com/thorproduct.cfm?partnumber=BSW25>. [Accessed 10 10 2018].
- [24] Thorlabs, "WG31050 - Ø1" Sapphire Broadband Precision Window, Uncoated," 2018. [Online]. Available: <https://www.thorlabs.com/thorproduct.cfm?partnumber=WG31050>. [Accessed 10 10 2018].
- [25] G. Bailet, "Method and device for detecting and assessing a thickness variation of a workpiece". WO Patent WO2018100256A1, 07 06 2018b.